One-pot chemo-enzymatic synthesis and one-step recovery of length-variable long-chain polyphosphates from microalgal biomass

Lin, Yi-Hsuan; Nishikawa, Shota; Jia, Tony Z.; Yeh, Fang-I; Khusnutdinova, Anna; Yakunin, Alexander; Fujishima, Kosuke; Wang, Po-Hsiang

Green Chemistry

Published: 27/10/2023

Peer reviewed version

One-pot chemo-enzymatic synthesis and one-step recovery of length-variable long-chain polyphosphates from microalgal biomass

Yi-Hsuan Lin[1,†], Shota Nishikawa[2,3,†], Tony Z. Jia[2,4], Fang-I Yeh[1], Anna Khusnutdinova[5], Alexander F. Yakunin[5], Kosuke Fujishima[2,6] and Po-Hsiang Wang[1,7*]

[1]Graduate Institute of Environmental Engineering, National Central University, Taoyuan, 320 Taiwan (R.O.C)
[2]Earth-Life Science Institute, Tokyo Institute of Technology, Tokyo 152-8550, Japan
[3]School of Life Science and Technology, Tokyo Institute of Technology, Tokyo 152-8550, Japan.
[4]Blue Marble Space Institute of Science, Seattle, Washington, USA
[5]Centre for Environmental Biotechnology, School of Natural Sciences, Bangor University, Bangor, LL57 2UW, United Kingdoms
[6]Graduate School of Media and Governance, Keio University, Fujisawa 252-0882, Japan
[7]Department of Chemical and Materials Engineering, National Central University, Taoyuan, 320 Taiwan (R.O.C)
[†]These authors contributed equally to this work.
[*]Correspondance: tommy.wang@elsi.jp

Keywords: Polyphosphate; microalgae; polyphosphate kinase; one-pot enzyme cascade; bioeconomy; biomass valorization.

Abstract

Phosphate, an essential ingredient in fertilizers and detergents used daily worldwide, is a finite resource that may be exhausted within 70 years, while improper phosphate waste disposal into aquatic environments will result in eutrophication. Despite some chemical-based methods, biological phosphorus removal using polyphosphate-accumulating organisms, such as microalgae, is a sustainable alternative to reclaim phosphate from wastewater before the wastewater enters aquatic environments, preventing ecosystem damage while recovering the phosphate for industrial use. Moreover, polyphosphates have profound biological functions and biomedical applications, serving as energy stock, drug delivery vesicles, coagulation factors, and antiviral agents depending on the length of the polyphosphate chain, showing inherent value in polyphosphate recovery. However, before this study, there were no sustainable and efficient approaches to synthesizing purified polyphosphates enriched with different lengths, which limited industrial and biomedical applications. Here, by leveraging the power of thermodynamic coupling and phase transitions, we established a one-pot, two-step multi-enzyme cascade (comprising creatine kinase and two polyphosphate kinases) to transform heterogeneous polyphosphate in microalgae biomass to insoluble long-chain polyphosphate 1,300-mers, allowing for further purification in single-step. In the cascade reactions, introducing creatine as the high-energy P-shuttle enables controlled manipulation of creatine kinase reaction direction *via* pH modulation, effectively circumventing competition between the two polyphosphate kinase-mediated reactions. Finally, we optimized a thermo-digestion approach to transform the polyphosphate 1,300-mers into shorter polyphosphates enriched with a narrow length range. Therefore, the processes established here create a sustainable P bioeconomy platform to refine microalgal biomass for biotechnological use.

Introduction

Phosphorus is a key element in the biomass of all living organisms [1] and is essential for modern agriculture/industry as a component in fertilizer, animal feed, and detergents [2]. However, the most accessible phosphorus exists in the form of lithosphere apatite minerals and is inaccessible to land-based plants, while worldwide phosphorus demand has been rapidly growing and is expected to exceed supply within 70 years due to rapid global population increase [3]. To increase the phosphorus supply, "wet process methods" have been invented to convert unusable inorganic phosphorus into phosphoric acid, a precursor to fertilizers, followed by an introduction to land plants [4]. However, excessive introduction of soluble phosphorus into aquatic environments is also detrimental [5], *e.g.*, phosphorus leakage from agricultural fields, wastewater plants, and household sewage triggers eutrophication in downstream aquatic environments [6]. Therefore, the sustainable recovery and reuse of phosphorus is urgently needed to sustain the global food chain and other human activities, while preserving aquatic environments.

Wastewater is an abundant, widespread phosphorus sink produced by a variety of agricultural and industrial activities. Phosphorus recycling from wastewater would not only prevent further downstream ecological damage but also lead to the development of a sustainable P bioeconomy, where recycled phosphorus can be converted into useful, value-added P-containing materials. In addition to well-established P removal methods, such as adsorption and chemical precipitation [7,8], biological phosphorus removal can occur through polyphosphate-accumulating organisms (PAOs) uptaking phosphorus from wastewater and accumulating the phosphorus in the form of inorganic polyphosphate (polyP) [9–12]; the accumulated polyP can subsequently be

extracted from microalgal cells for downstream application [13]. These examples suggest that biological phosphorus removal systems are eco-friendly and cost-effective, making them good candidates for developing the sustainable P bioeconomy.

PolyP has numerous biological functions and biomedical applications, which vary depending on chain length (**Figure 1**) [14,15]; short/medium-chain polyP (10–100-mer) promotes bone regeneration [16], wound healing [17,18], and blood coagulation [19,20], while long-chain polyP (100–1,000-mer) are less soluble (>300-mer is insoluble)[21] and can be used as biomolecule-carrying microdroplets that exhibit antiviral properties [22–24] or as molecular chaperones [25]. Traditionally, phosphate glass, composed of polydisperse polyP, is synthesized by heating phosphoric acid at high temperatures (>700°C) [26]. The chemically synthesized polyP is then partially hydrolyzed by the alkaline treatment and separated by length *via* liquid chromatography or fractional precipitation using organic solvents, which are resource and time-intensive [27], along with low yields of polyP of each specific length. Similar to chemical methods, polyP purified from microalgal systems is also polydisperse [28], which also requires separation and harvesting for downstream use. Thus, for microalgal phosphate removal systems to be included within the sustainable P bioeconomy, the development of a sustainable method to produce length-variable polyP of higher homogeneity is necessary.

As polyP is ubiquitous in biology and because polyP function varies depending on chain length, organisms must harbor some biochemical mechanisms to produce polyP of a specific length to achieve their physiological goals. In prokaryotes, the biosynthesis and utilization of polyP are primarily mediated by polyP kinases (PPKs) with the two main families represented by PPK1s

and PPK2s, which catalyze the reversible transfer of phosphate between polyP and nucleotides [29]. Recent phylogenetic analysis has identified three subtypes of PPK2s (class I, II, and III) [30,31]; class I and II PPK2s catalyze the polyP-driven phosphorylation of either NDP or NMP, respectively, while class III PPK2s can phosphorylate both NDP and NMP, enabling direct NTP production from NMP [32]. Class I and II PPK2s have been used for *in vitro* biosynthesis of acetone [33], aldehyde [34], and thiamine phosphates [35] as well as biocatalytic regeneration of S-adenosyl-L-methionine [36], while class III PPK2s have been used for cell-free protein synthesis and *in vitro* biocatalytic reactions that simultaneously require regeneration of both ATP and GTP [37]. In the PPK2-mediated A(G)TP regeneration system, long-chain polyP (100-mer), as opposed to short-chain polyP at the same molar content of total orthophosphate, can significantly enhance cell-free protein yield.

Inspired by biology, we aimed to develop a sustainable mechanism to synthesize length-variable long-chain polyP. Given that *Cytophaga* PPK2 can use polydisperse polyP to phosphorylate ADP to ATP, while *Ralstonia eutropha* PPK2c can catalyze the direct synthesis of insoluble long-chain polyP (length undetermined) from ATP without a priming short-chain polyP [38,39], we harnessed these two PPK2 enzymes in tandem to convert polydisperse polyP in wastewater microalgae biomass into insoluble long-chain polyP 1,300-mer with creatine as the P-shuttle (**Table 1**). The insoluble long-chain polyP 1,300-mer then can be purified by a simple one-step filtration (phase transition), followed by non-enzymatic degradation to yield length-variable polyP enriched with varying shorter lengths.

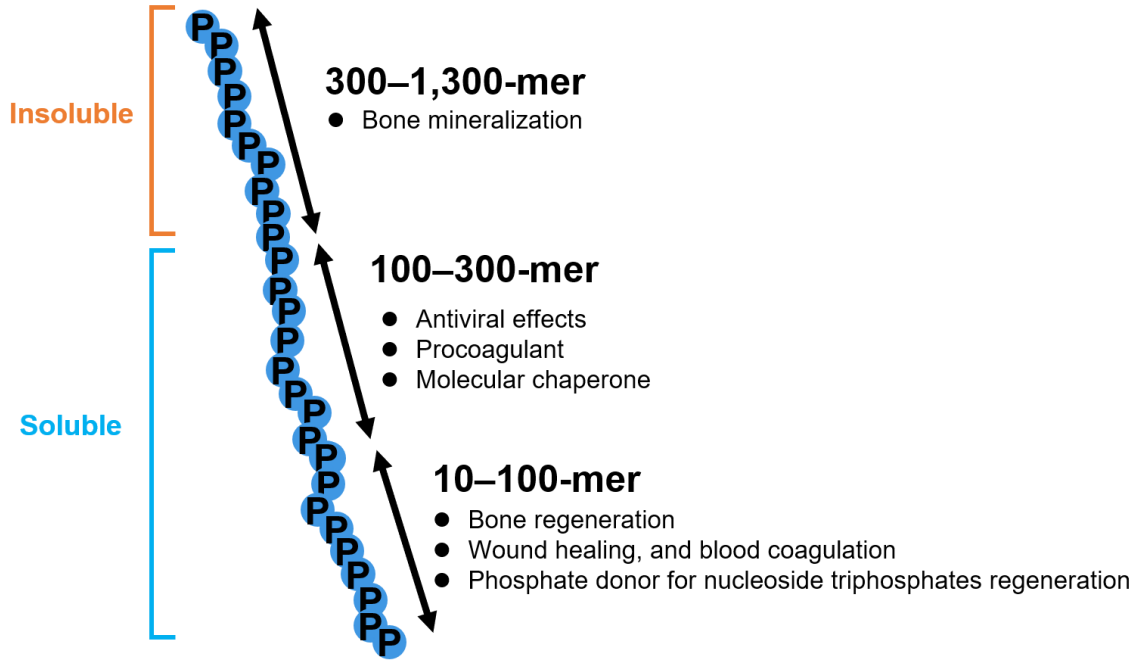

Figure 1. Functional diversity of polyphosphates of different lengths.

Experimental section

For full experimental details please refer to the ESI. Unless specified otherwise, chemicals and reagents are purchased from Sigma-Aldrich (St. Louis, MO, USA). Enzyme kinetics and sources of the recombinant enzymes used in this study are provided in **Tables S1** and **S2** in **Supplementary Information**. Sodium dodecyl sulfate-polyacrylamide gel electrophoresis (SDS-PAGE) gel images of the purified recombinant enzymes; HPLC chromatograms of creatine phosphate and creatine; standard curves of NAD(P)H, creatine phosphate, polyphosphate, and

ATP; and the geographical coordinate of the P-rich wastewater-sampling site are available in **Appendix**.

Quantification of polyP using the toluidine blue O (TBO) method

PolyP was quantified by a metachromatic assay with the TBO method using commercial polyP (sodium polyP (~25-mer); Sigma-Aldrich) as a standard. The TBO method is based on the concentration-dependent decrease in $\lambda_{630\ nm}$ by the metachromatic reaction of TBO with polyP [40]. Briefly, sample solution (5 µL) was mixed with TBO assay solution (250 µL; 15 µg/mL) and acetic acid (0.1 N) at room temperature [41]. Then, $\lambda_{630\ nm}$ was measured for the TBO-treated sample in a microplate spectrophotometer for 10 min (Molecular Devices/Spectra Max® iD3, San Jose, CA, USA). The $\lambda_{630\ nm}$ was later converted into polyP concentration based on standard curves derived from the different commercial sodium polyP standard concentrations. The standard curves of polyP concentrations are available in the **Appendix**.

Microalgae cultivation under nitrogen-deficient conditions

Microalgae *Chlorella vulgaris* (*C. vulgaris*) was purchased from the Bioresource Collection and Research Center (Hsinchu, Taiwan), which was cultivated in heat-sterilized wastewater collected from the discharge of a local piggery wastewater treatment plant with continuous daylight exposure (**Appendix**). *C. vulgaris* was cultivated in 2 L Erlenmeyer flasks containing the sterilized wastewater (1 L; pH adjusted to neutral) at room temperature with continuous shaking (200 rpm) for aeration and to prevent microalgae from sticking to the bottom of the flask as previously described [42].

148 ***Epifluorescence microscopic detection of polyP***

149 PolyP was detected by epifluorescence microscopy as previously described [38]. Briefly, polyP
150 granules were stained with DAPI (4′,6-diamidino-2-phenylindole) (0.1 mg/mL in distilled H_2O)
151 for at least 10 min and the stained granules were visualized by epifluorescence microscopy on an
152 oil objective at 1,000 x magnification (ZEISS/AXIOSKOP 2, Oberkochen, Germany).

153 ***In vivo polyP visualization using TBO staining***

154 *C. vulgaris* cells were air-dried and heat-fixed on a glass slide (76 × 26 mm; Thickness 1.2–1.5
155 mm). Intracellular polyP granules were then stained with TBO (15 mg/L) for 10 min by
156 submerging the whole glass slide (containing the fixed cells) into TBO solution. The slide was
157 then gently washed with double distilled H_2O, followed by air drying for 15 min and subsequent
158 observation by an optical microscope at 100 x magnification (Olympus CX21FS1, Shinjuku,
159 Tokyo, Japan).

160 ***C. vulgaris cell lysis and partial polyP purification***

161 The *C. vulgaris* cells were disrupted and partially purified as previously described [40]. *C. vulgaris*
162 biomass was collected by centrifugation at 4,430 × g for 10 min at room temperature and then
163 resuspended in buffer (HEPES-K (pH 7.0; 20 mM), KCl (0.15 M), and ethylenediaminetetraacetic
164 acid (EDTA) (5 mM)) at a pellet to buffer ratio of 1:3. The cells were lysed *via* ultrasonication for
165 20 min (3 s on and 3 s off) and the cell-lysate containing polyP was subsequently incubated at
166 100°C for 10 min, followed by centrifugation at 8,000 × g for 3 min at room temperature to separate
167 the cell debris from the supernatant containing the polydisperse polyP. The polyP concentration
168 within the supernatant and the initial microalgal wastewater were quantified by the TBO method

(see above). The supernatant containing polyP was stored at –80°C for further use in subsequent experiments.

ATP regeneration using polydisperse microalgal polyP

Polydisperse polyP in the microalgal cell-lysate was used for ATP regeneration using the *Cytophaga* PPK2. In the phospho-transfer reaction, the theoretical product is ATP and polyP with one less unit in the chain ($polyP_{(n)} + ADP \rightarrow polyP_{(n-1)} + ATP$). To measure the reaction kinetics for stoichiometric analysis, ATP production was monitored by both ***(i)*** the time-dependent consumption of polyP using the TBO method (see above) and ***(ii)*** the hexokinase/glucose-6-phosphate dehydrogenase (Roche, Basel, Switzerland)-coupled $NADP^+$ reduction process ($\lambda_{340\ nm}$) as described previously [37]. In the coupled HK/G6PD enzyme cascade, glucose is first converted into glucose-6-phosphate by HK using one ATP, which is then converted into dehydro-glucose-6-phosphate, along with the reduction of one $NADP^+$ to produce one NADPH, which can be observed through $\lambda_{340\ nm}$. The reaction mixtures (200 µL) contained Tris-HCl (pH 7.0; 100 mM), Mg^{2+} (10 mM), microalgal polyP (1.5–10 mM), adenosine (1–3 mM), and *Cytophaga* PPK2 (0.08 mg/mL). The reaction was initiated by the addition of PPK2 and the ATP production was monitored at 37°C for 10 min by measuring the ATP-dependent $NADP^+$ reduction through the increase in $\lambda_{340\ nm}$.

Enzymatic synthesis of creatine phosphate from polydisperse polyP in microalgal cell-lysate

A two-enzyme cascade comprising *Cytophaga* PPK2 and rabbit creatine kinase (CK) (Sigma-Aldrich) was applied to sequentially convert the microalgal polyP into creatine phosphate *via* ATP. The optimized reaction mixtures (200 µL) contained Tris-HCl (pH 9.0; 0.1 M), $MgSO_4$ (10 mM), microalgal polyP (10 mM), creatine (50 mM), ATP (1 mM), N-acetyl-L-cysteine (2 mM),

Cytophaga PPK2 (0.3 mg/mL), and CK (0.03 mg/mL); different conditions, including pH 8.0, 5 mM and 15 mM $MgSO_4$, and 10–40 mM creatine were also tested, but the reported reaction conditions are the optimized conditions (10 mM Mg^{2+}, 5 mM microalgal polyP, and 50 mM creatine at pH 9.0 in Tris buffer) for the greatest amount of creatine phosphate conversion (~4.75 mM; 95% yield), which were used for all subsequent experiments. The reaction was initiated by the addition of *Cytophaga* PPK2 and CK, and the formation of creatine phosphate was monitored at 30℃ for 30 min by the consumption of the microalgal polyP using the TBO method (see above) as well as HPLC analysis.

Enzymatic synthesis of insoluble polyP 1,300-mer

Another two-enzyme cascade comprising *Ralstonia* PPK2c (polyP-synthesizing) and rabbit CK was used to sequentially convert creatine phosphate into homogeneous polyP 1,300-mer *via* ATP. The formation of the polyP 1,300-mer was monitored by the TBO method (see above). The reaction mixtures (200 μL) contained (HEPES-K (pH 7.0; 90 mM), Tris-HCl (pH 7.0; 10 mM), $MgSO_4$ (10 mM), creatine phosphate (5 mM), ATP (3.5 mM), PPK2c (0.5 mg/mL), and CK (0.1 mg/mL); different ATP concentrations (1–5 mM) were also tested, but the reported reaction conditions are the optimized conditions used for all subsequent experiments. The reaction was initiated by the addition of CK and *Ralstonia* PPK2c at 30℃ and the formation of the polyP 1,300-mer was monitored *via* the time-dependent decrease in $\lambda_{630\ nm}$ using the TBO method.

Degradation of insoluble polyP 1,300-mer by non-enzymatic hydrolysis

The synthesized polyP 1,300-mer in the microalgal cell-lysate was collected by filtration using a 0.45-μm MF-Millipore® membrane filter paper (Burlington, Massachusetts, USA) along with a vacuum pump. The remainder was washed by ddH_2O until the intensity of $\lambda_{265\ nm}$ (indicative of

N(M/D/T)P) and $\lambda_{280\ nm}$ (indicative of protein/polypeptide) of the flowthrough decreased to background levels. After resuspension of the reaction by adding 300 µL HEPES-K buffer (25 mM; pH 7.5), the reaction mixture ($MgSO_4$ (5 mM), EDTA (5 mM), and polyP 1,300-mer (5 mM)) was subjected to time-dependent hydrolysis at 95°C.

Results

Polydisperse polyP extraction from wastewater microalgal biomass

To develop the sustainable P bioeconomy process, we selected wastewater discharge samples collected from a local piggery as a substrate for microalgae cultivation and polyP production (**Figure 2A**). *Chlorella vulgaris* was cultivated in heat-sterilized wastewater discharge under nitrogen-deficient conditions to induce phosphorus assimilation in the form of polyP [43]. After cultivation, TBO was used to live-stain the microalgal cells and *in vivo* visualize the accumulation of small purple-stained particles within the cells, approximately 1 µm in diameter, which were likely highly enriched in polyP (**Figure 2B**). The polyP-accumulating microalgal biomass was then collected by centrifugation and lysed by sonication in an ice bath, followed by heating at 100°C with the EDTA to prevent non-enzymatic polyP degradation (**Figures 2C and S1AB**). The heating step significantly enhanced the extraction efficiency and prevented enzymatic polyP degradation, resulting in microalgal cell-lysates containing up to 35 mM polyP (**Figure 2D**). Thus, microalgal polyP in the form of heterogeneous solid particle-like structures (**Figure 2E**) can be collected using simple cultivation and extraction. Moreover, the cell-lysate polyP appeared to be polydisperse in length (**Figure 2F**).

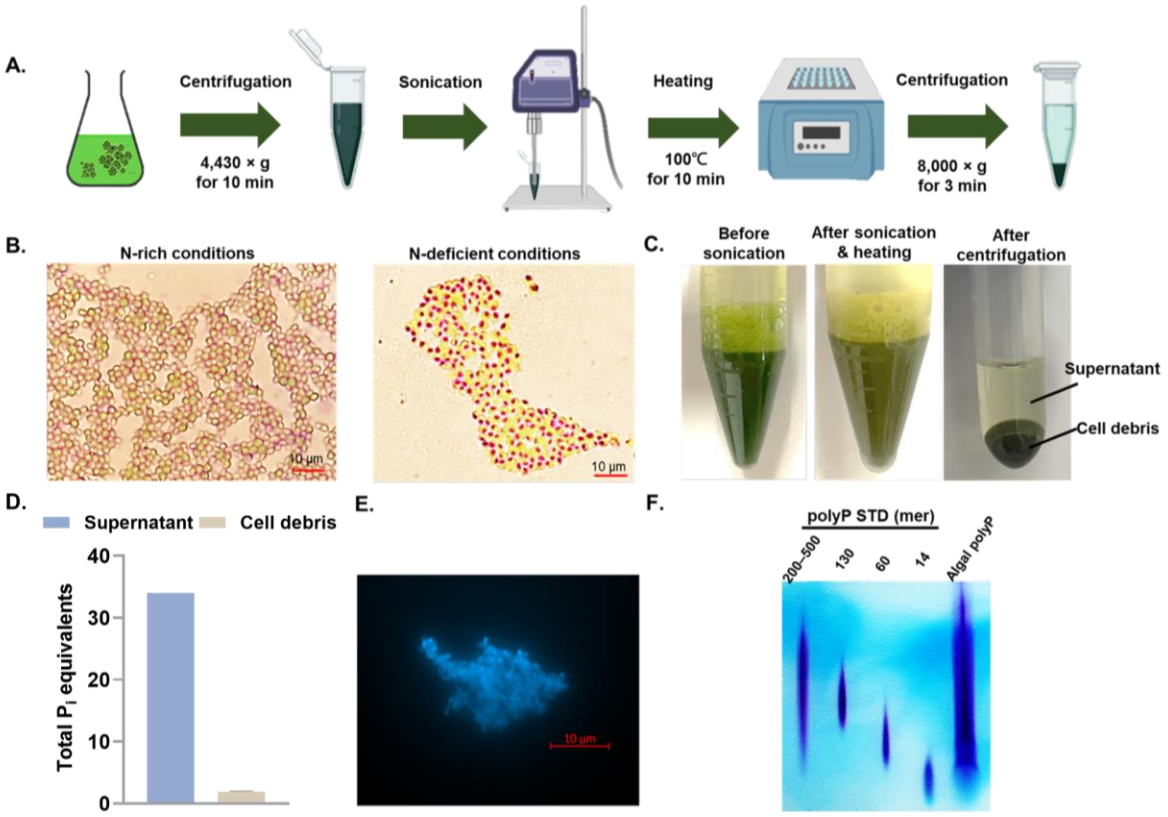

Figure 2. Microalgae cultivation and partial fractionation of the accumulated polyphosphate (polyP). (A) The overall scheme for producing polydisperse microalgal polyP. **(B)** PolyP accumulation in *Chlorella vulgaris* cultivated in sterilized wastewater under nitrogen-deficient conditions. The intracellular polyP was visualized *in vivo* by TBO staining and analyzed by optical microscopy. **(C)** Production of the polyP-rich cell-lysate (supernatant) from microalgal biomass *via* sonication, heating, and centrifugation. **(D)** The soluble polyP concentrations (shown in total P_i equivalents) in the supernatant and the cell debris (measured by the TBO assay). Error bars represent the standard deviation from three experimental replicates. **(E-F)** DAPI-stained epifluorescent microscopy analysis (**E**) and TBE-Urea polyacrylamide gel electrophoresis (6%, w/v) analysis (**F**) of the granular polydisperse polyP aggregates.

Polydisperse microalgal polyP as P-donor for PPK2-mediated ATP regeneration

The next step for the proposed sustainable P bioeconomy was to convert the polydisperse microalgal polyP to another P-containing molecule (creatine phosphate) for the downstream synthesis of homogeneous long-chain polyP. However, the prerequisite of this step is that the microalgal cell-lysate polyP can serve as the substrate of *Cytophaga* PPK2, similar to the case with commercial polyP 25-mers (**Figure S2**), so that the high-energy phosphate can be completely transferred to the downstream P-carrier. To measure the reaction kinetics to confirm complete P transfer from polyP to produce ATP, we coupled the *Cytophaga* PPK2-mediated ATP production process to an NADP reduction process driven by an enzyme cascade consisting of hexokinase (HK) and glucose-6-phosphate dehydrogenase (G6PD) (**Figure 3A**). Upon incorporation of the HK/G6PD cascade to the *Cytophaga* PPK2-mediated ATP production process, we observed NADPH accumulation over time upon progression of this reaction in the microalgal cell-lysate (**Figure 3B**); stoichiometric analysis also confirmed that NADPH production (*i.e.*, ATP regenerated) is equivalent to polyP consumption, suggesting that all high-energy phosphate contained within polyP was transferred fully to produce ATP (**Figure 3C**).

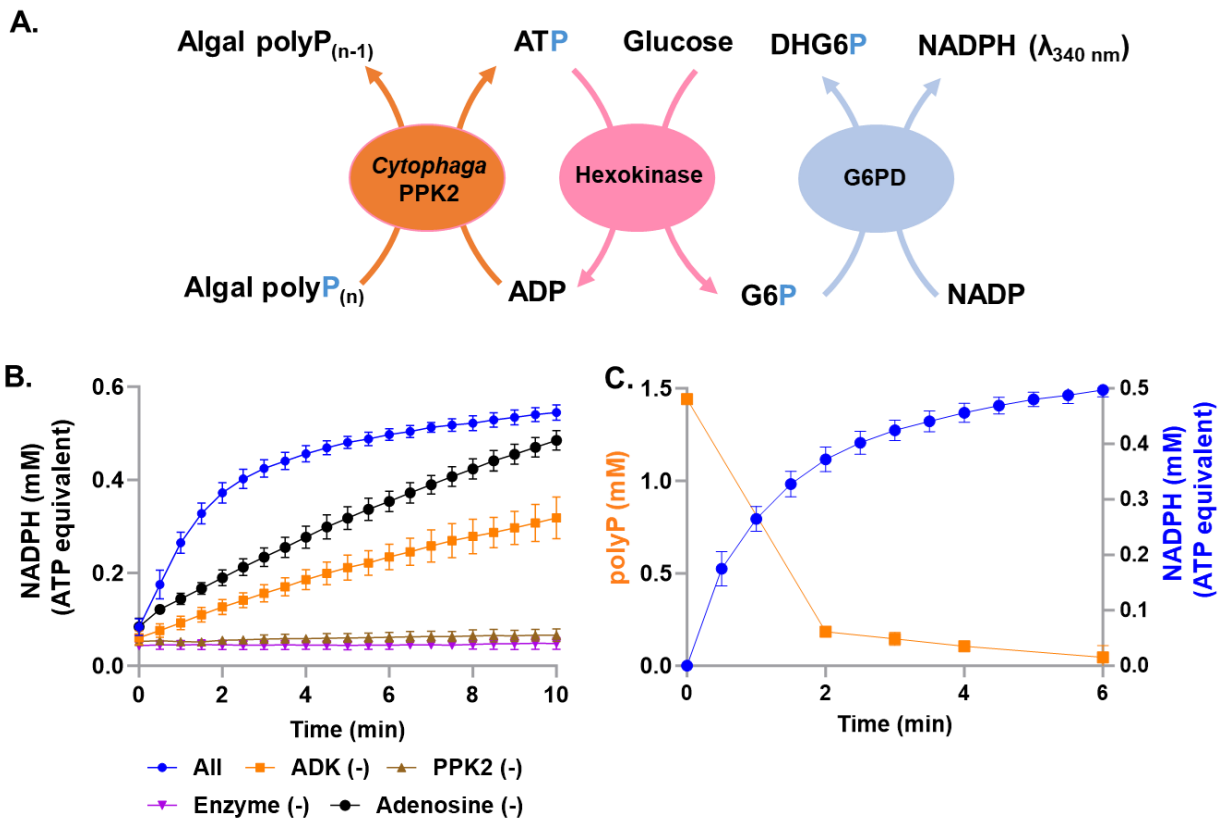

Figure 3. *Cytophaga* PPK2-based ATP regeneration using polydisperse polyP in microalgal cell-lysate. (A) Schematic diagram showing the enzymatic cascade of the *Cytophaga* class III PPK2 and HK-G6PD-coupled NADPH production assay. HK; hexokinase, G6PD; glucose-6-phosphate dehydrogenase, DHG6P; dehydroglucose-6-phosphate. **(B)** PolyP-based ATP regeneration monitored by ATP-dependent NADPH production ($\lambda_{340\ nm}$) using G6PD-HK. **(C)** Stoichiometric analysis of *Cytophaga* PPK2-dependent polyP consumption and ATP-dependent NADPH production by HK-G6PD. The concentrations of the consumed polyP and produced NADPH were monitored through the TBO assay and at $\lambda_{340\ nm}$, respectively. The error bars represent the range and the data points represent the average from two independent experimental replicates.

Stepwise conversion of polydisperse microalgal polyP into insoluble long-chain polyP 1,300-mer

We then chose creatine phosphate as the P-carrier for downstream synthesis of insoluble long-chain polyP (**Figure 4A; Table 1**), as eQuilibrator-based free energy calculations suggest that CK-mediated phospho-transfer from ATP to creatine is thermodynamically favorable at basic pH (**Figures 4B** and **S3A**) [44]. Given the previous demonstration that P from microalgal polyP can be fully converted to ATP, complete phospho-transfer from the polydisperse polyP to creatine *via* ATP in the microalgal cell-lysate is plausible. On the other hand, the CK-mediated phospho-transfer from creatine phosphate to ADP (the reverse reaction) is thermodynamically favorable at neutral pH (**Figure S3B**). Therefore, by modulating the pH of the microalgal cell-lysate, we attempted to first convert the polydisperse polyP and creatine into creatine phosphate *via* ATP ($polyP_{(n)}$ + creatine → $polyP_{(n-1)}$ + creatine phosphate) using polyP-consuming *Cytophaga* PPK2 and CK at basic pH, and later convert creatine phosphate back into long-chain polyP and creatine using CK and polyP-synthesizing *Ralstonia* PPK2c *via* ATP at neutral pH ($polyP_{(n)}$ + creatine phosphate → $polyP_{(n+1)}$ + creatine). Using free energy calculations as a guide (**Figure S3**), we optimized the conditions of the two-enzyme PPK2/CK cascade (**Figure 4A**). The greatest polyP consumption and creatine phosphate production were observed with 10 mM Mg^{2+} at pH 9.0 (**Figures 4C** and **S4A–E**), while 5 mM microalgal polyP also resulted in nearly complete polyP consumption (**Figure 4D**).

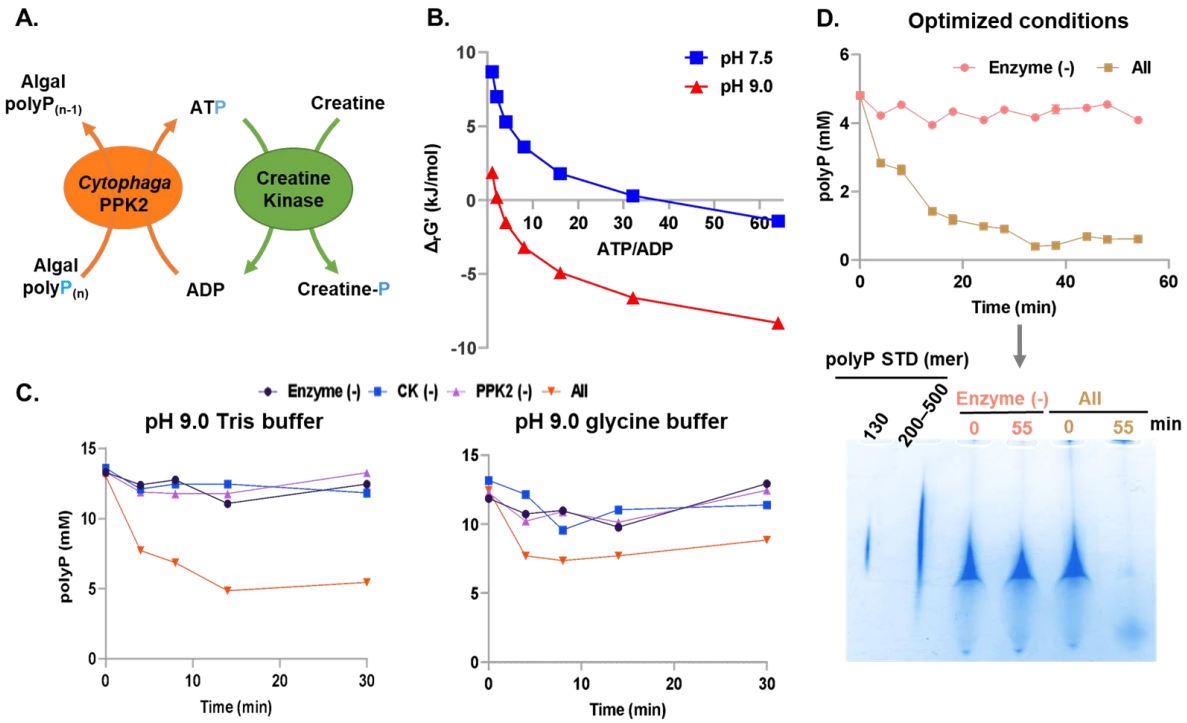

297

298 **Figure 4. Conversion of polydisperse microalgal polyP into creatine phosphate *via* ATP by**
299 **the enzymatic cascade comprising CK and *Cytophaga* PPK2. (A)** Schematic diagram showing
300 the PPK2-CK enzyme cascade. **(B)** eQuilibrator-based thermodynamic calculations of creatine
301 phosphorylation at circumneutral (pH 7.5) or alkaline (pH 9.0) pH. **(C)** Time-dependent creatine
302 phosphate production by the PPK2-CK cascade in Tris-HCl or glycine buffer at pH 9.0. The
303 production of creatine phosphate was monitored by the consumption of the polyP *via* TBO assay.
304 **(D)** Time-dependent creatine phosphate production by the PPK2-CK cascade under optimized
305 conditions (Tris-HCl (pH 9.0), Mg^{2+} (10 mM), creatine (50 mM), and microalgal polyP (5 mM)).
306 The reactions were conducted with and without *Cytophaga* PPK2. The nearly complete
307 consumption of polyP was verified *via* quantitative TBO measurements (top) from TBE-Urea
308 polyacrylamide gel electrophoresis analysis (bottom).

309

310

Next, we sought conditions to transfer the high-energy phosphate from creatine phosphate to build a growing polyP chain. Thus, we then applied a two-enzyme cascade containing CK and *Ralstonia* PPK2c in HEPES-K at neutral pH with ATP as the P shuttle (pH 7.0); the high-energy phosphate from creatine phosphate is transferred to ADP *via* CK (regenerating ATP), while the *Ralstonia* PPK2c transfers the high-energy phosphate on the regenerated ATP onto a growing polyP chain (**Figure 5A**). After optimization through a combination of free energy calculations and experiments, efficient conversion of the creatine phosphate into polyP *via* the CK/PPK2c cascade was successfully demonstrated with the initial addition of 3.5 mM ATP **(Figures 5B and S3B)**. In the absence of creatine phosphate (but with added ATP), nearly no long-chain polyP was produced, suggesting the importance of creatine phosphate to drive the aforementioned exergonic phospho-transfer (thermodynamic coupling) **(Figure S5)**.

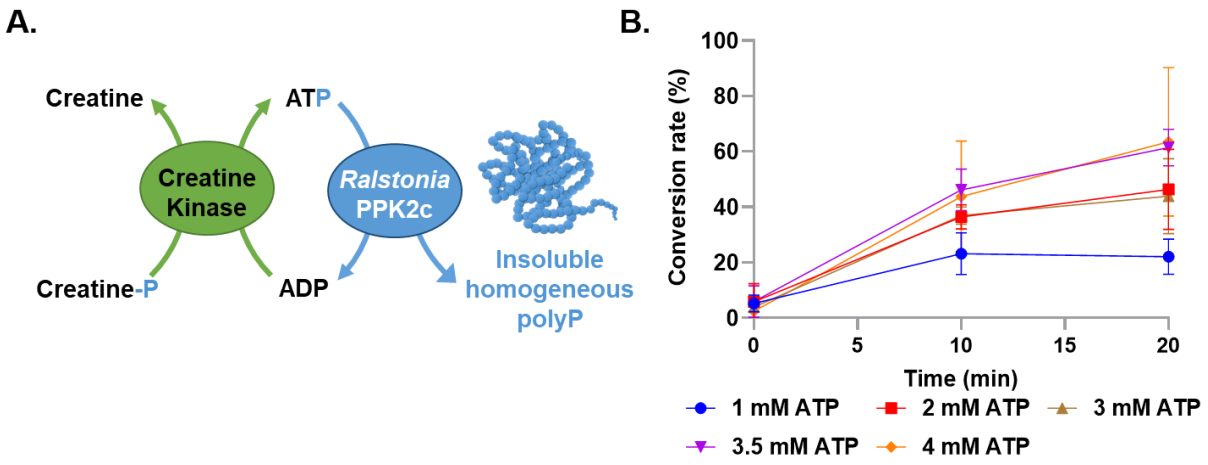

Figure 5. Conversion of creatine phosphate into homogeneous insoluble long-chain polyP *via* ATP by the enzymatic cascade comprising CK and *Ralstonia* PPK2c. (A) Schematic diagram showing the two-enzyme cascade comprising CK and *Ralstonia* PPK2c for homogeneous insoluble long-chain polyP production. **(B)** Time-dependent long-chain polyP production by the CK-PPK2c cascade in HEPES-K buffer (pH 7.5) with varying ATP concentrations. Error bars represent the standard deviation and the data points represent the mean from three independent experimental replicates.

One-pot enzymatic synthesis and one-step recovery of insoluble long-chain polyP 1,300-mer from polydisperse polyP

Next, given that both enzymatic cascades (*Cytophaga* PPK2-CK and CK-*Ralstonia* PPK2c) were shown separately to be effective to convert the polydisperse microalgal polyP into long-chain polyP *via* creatine phosphate, we then sought to perform the entire reaction in a one-pot, two-step fashion for greater throughput and scalability. Specifically, we first applied the creatine phosphate-producing cascade (*Cytophaga* PPK2-CK) at pH 9.0 (**Figure 6A**), followed by the removal of *Cytophaga* PPK2 and adjustment of the reaction pH to neutral (**Figure 6B**) and addition of *Ralstonia* PPK2c to transform the produced creatine phosphate to ATP and then to the long-chain polyP (**Figure 6C**). However, our experimental analysis revealed that the two cascades require completely different buffer systems at the required pH range (pH 7.0–9.0) to be active. Thus, we reasoned that a mixture of buffers amenable to each cascade at an intermediate pH may facilitate both cascades in the same pot, albeit possibly with sub-optimal efficacy for either or both cascades. Among all conditions tested, a HEPES-K:Tris-HCl ratio of 8:1 resulted in the greatest long-chain polyP production (**Figures S6A–E**). In parallel, we observed a nearly complete conversion of the creatine phosphate into long-chain polyP and creatine by the CK-*Ralstonia*

PPK2c cascade under the same assay conditions but in the HEPES buffer **(Table 2)**, suggesting that the mixed buffer is indeed sub-optimal for the CK-*Ralstonia* PPK2c cascade. However, considering that the *Cytophaga* PPK2-CK cascade requires completely different conditions, the mixed buffer conditions can still produce long-chain polyP at a high yield (90%) through a one-pot, two-step process.

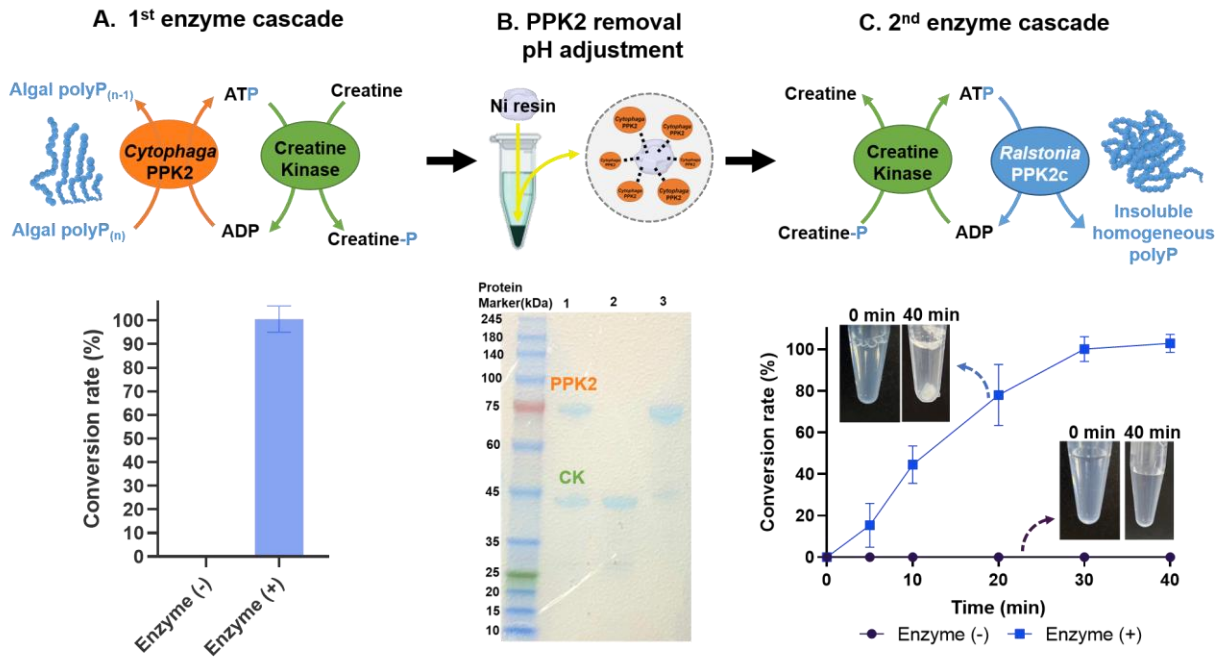

Figure 6. One-pot, two-step enzymatic synthesis of homogeneous insoluble long-chain polyP from polydisperse microalgal polyP. (A) Conversion of polydisperse microalgal polyP into creatine phosphate *via* the *Cytophaga* PPK2-CK cascade. **(B)** The removal of His-tagged *Cytophaga* PPK2 from the microalgal cell-lysate (verified by SDS-PAGE) using the Ni-chelating resin. 1: the cell-lysate with both *Cytophaga* PPK2 and CK; 2: the cell-lysate after *Cytophaga* PPK2 removal by a Ni-chelating resin; 3: the elution of the Ni-chelating resin used for *Cytophaga* PPK2 removal. A trace amount of CK was also co-eluted. **(C)** Conversion of creatine phosphate into homogeneous insoluble long-chain polyP solids *via* the CK-*Ralstonia* PPK2c cascade. The

conversion rates of the insoluble long-chain polyP synthesis reaction with the mixed buffer system were calculated at different time points. The reactions were conducted with and without *Ralstonia* PPK2c. Error bars represent the standard deviation and the data points represent the mean from three independent experimental replicates.

We also observed insoluble material produced after the one-pot, two-step enzymatic cascade (**Figure 6C**). As polyP >300-mer is generally insoluble, which we conjectured was the chain length of the polyP product. After filtration using a 100-kDa cutoff centrifugal filters, the polyP products appeared to be all "ultra" long-chain polyP (>100-kDa or >1,000-mer), which was highly homogeneous and in the 1,300-mer unit range (**Figure 7A and S7AB**). This is in contrast to the polydisperse polyP in microalgal cell-lysate before the enzymatic catalysis, which has roughly equal concentrations of polyP of sizes larger and smaller than 100 kDa (**Figure 2F**). Prior to this study, long-chain polyP 700-mer was referred to as "super long-chain" polyP; however, our enzymatically synthesized homogeneous polyP product is nearly twice as long compared to the longest commercially available polyP.

Although homogeneous long-chain polyP has been produced *via* our one-pot, two-step enzymatic cascades, the product could potentially contain some byproducts or contaminants, such as nucleic acids and peptides, that would inhibit downstream use or processing for industrial purposes. We thus further subjected the microalgal cell-lysate containing the polyP 1,300-mer product to a protease treatment and filtration by a 0.45-µm filter for polyP purification.

Consistently, ATP and proteins (indicated by $\lambda_{260\text{-}280\ nm}$) were nearly completely removed (**Figures 7B and S7C; Table 2**), suggesting effective purification of the polyP 1,300-mer product. After filtration, we then dried the remainder, which resulted in a white powder that fluoresced after DAPI-staining, confirming its composition to be of polyP (**Figure 7A**).

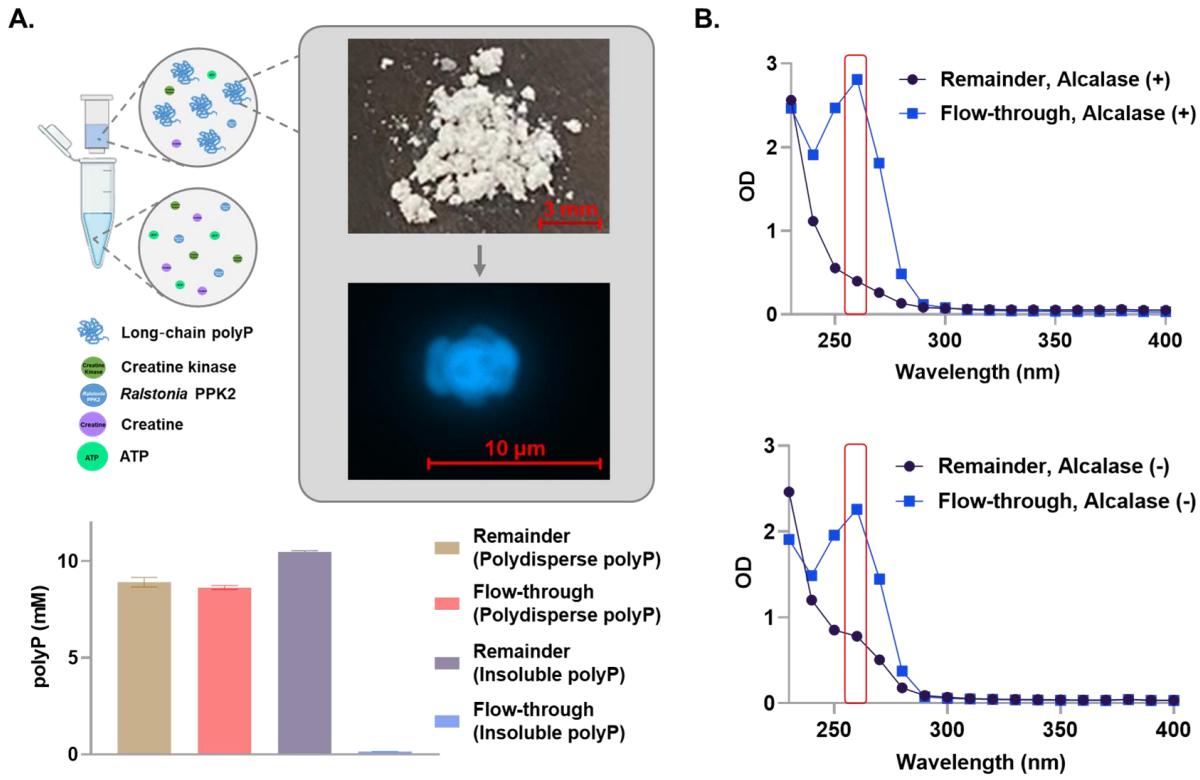

Figure 7. Purification of long-chain polyP using a membrane filter after the protease digestion. (A) The solutions containing the polydisperse microalgal polyP or the insoluble homogeneous long-chain polyP obtained from the one-pot, two-step enzymatic cascades were subjected to filtration through a 100-kDa filter. PolyP concentrations in the remainder and flow-through fractions were quantified by the TBO assay. **(B)** Removal of small molecules (ATP, creatine, and salts) and proteins from the remainder fraction (verified by UV-Vis analysis). The reaction mixture containing insoluble long-chain polyP was subjected to filtration before and after the proteolysis treatment.

Non-enzymatic production and application of length-variable polyphosphates from homogeneous long-chain polyP

While the goal of this study was to convert polydisperse polyP in wastewater microalgae biomass into insoluble and homogeneous long-chain polyP, we next wondered whether the developed process could lead to more value-added products aside from the polyP 1,300-mer. As mentioned previously, polyPs of different lengths have different functional properties, and the ability to acquire polyPs of different lengths is of particular value. Before this study, industrial production methods for polyP of different chain lengths were time-, resource-, cost-, and organic waste-intensive. Thus, to produce a shorter homogeneous polyP, we first subjected the polyP 1,300-mer to enzymatic treatment by exopolyphosphatase (PPX) [45]. However, rather than the polyP product length decreasing over time, the polyP concentration instead decreased over time (**Figure S8A**). Moreover, the treatment of polyP 1,300-mer with polyP-consuming *Cytophaga* PPK2 also resulted in a similar result (**Figure S8B**). We attribute this to the fact that PPX and *Cytophaga* PPK2 likely degrade single polyP chains fully before moving on to the next chain. Therefore, such an enzymatic degradation strategy was not amenable to our goals.

We thus decided to search for a non-enzymatic strategy for polyP length shortening that did not degrade single polyP chains fully. As Mg^{2+} is a known catalyst for non-enzymatic ATP

hydrolysis [46], we next subjected the polyP 1,300-mer to non-enzymatic digestion by Mg^{2+}, along with Mg^{2+}-chelating EDTA to slow down non-enzymatic polyP endo-cleavages. Our data revealed that the length of the polyP products was slightly reduced in a time-dependent manner at 70°C (**Figure 8A**); however, even after 4 hours of incubation, the size of the polyP products was still quite large (and the chain length remained much higher than the polyP 200–500-mer marker). Thus, we decided to increase the reaction temperature to 95°C. Over just one hour, the polyP length was reduced in a time-dependent manner, ultimately reaching a length on the order of 100-mer, while passing through the entire range of polymer lengths between 100–1,300-mer (**Figure 8B**). Moreover, the overall polyP concentration remained greater than 90% after the non-enzymatic hydrolytic process, confirming this process to be efficient with minimal loss of polyP product (**Figure 8C, Table 2**). Thus, polyP mixtures enriched with a narrow length range between 100–1,300-mer can be produced in high yield from the polyP 1,300-mer obtained from our enzymatic method, something hardly achievable with other synthetic polyP methods developed previously. The overall percentage yield of polyP 100-mer via our novel process is ~76%, which is ~2.5 times higher than the reported percentage yield of polyP via the traditional route (~30%), along with a 4–7 times lower carbon footprint than the traditional routes (**Table S3**). Therefore, the chemo-enzymatic process developed in this study is also highly "green" based on the green metrics.

As mentioned previously, our prior study revealed that PPK2 is more efficient in utilizing a polyP 100-mer than commercial short-chain polyP (25–65-mer) for ATP regeneration (at the same phosphate molar content). Thus, to demonstrate the added value of the non-enzymatic hydrolytic polyP 100-mer product while confirming its activity, we used the polyP 100-mer

product to perform the *Cytophaga* PPK2-based ATP regeneration process. Indeed, we observed more efficient ATP regeneration in the assays using the polyP 100-mer product than those using the commercial short-chain polyP (**Figure 8D**), suggesting the added value of the produced polyP 100-mer. We also note that other than the 100-mer, polyP of other lengths that are non-enzymatically generated from the homogeneous 1,300-mer, especially those between 100-mer and 300-mer, could also be used for biomedical applications (**Figure 1**). Altogether, the entire chemo-enzymatic system presented herein has resulted in a sustainable P bioeconomy platform valorizing low-value biomass waste to produce high-value products.

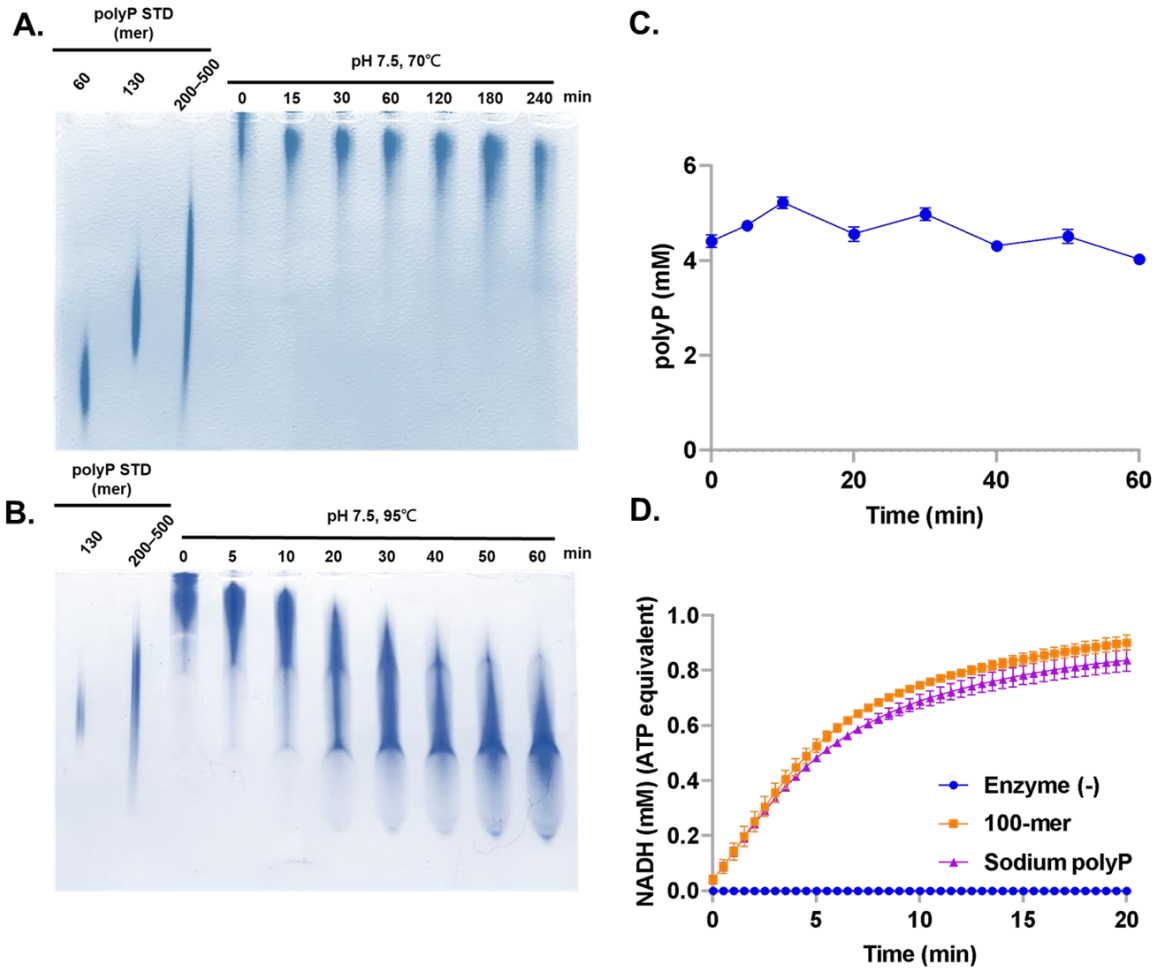

454

455 **Figure 8. Time-dependent thermo-digestion of a homogeneous polyP 1,300-mer by non-**
456 **enzymatic hydrolysis. (A-B)** The polyP 1,300-mer was incubated at **(A)** 70°C and **(B)** 95°C and
457 at pH 7.5, along with 5 mM Mg^{2+} and 5 mM ethylenediaminetetraacetic acid. The reaction
458 mixtures collected at different time points were analyzed by TBE-Urea polyacrylamide gel
459 electrophoresis, along with commercial polyP standards as a reference for the lengths. **(C)** The
460 total concentration of polyP (based on the molar content of orthophosphate) during the time-
461 dependent thermo-digestion was monitored by TBO assay. **(D)** HK-G6PD-mediated NADPH
462 production, which was coupled to *Cytophaga* PPK2-mediated ATP regeneration; commercial
463 short-chain polyP and purifiedpolyP 100-mer product was the high-energy phosphate donor
464 (normalized to the same molar content of orthophosphate). Error bars represent the standard
465 deviation and the data points represent the mean from three independent experimental replicates.

Discussion

In this study, we devised an efficient enzyme cascade to sustainably produce polyP 1,300-mer from wastewater microalgal biomass (or from commercial short-chain polyP). This technology simultaneously purifies wastewater to avoid eutrophication of downstream aquatic environments (**SDG 6**), while also mitigating the global phosphorus deficit and producing high-value biomedical materials following non-enzymatic hydrolysis (**SDG 3**). From a biochemical standpoint, the success of this technology results from the unusual properties of (***i***) CK that allow a pH-based modulation of the direction of polyP-ATP phospho-transfer (thermodynamic coupling) and (***ii***) *Cytophaga PPK2* and *Ralstonia* PPk2c that allow a two-step back-and-forth polyP phospho-transfer. However, this technique also succeeds due to a unique phase-transition property of the polyP reactants and products. In biology, phase transitions have often been employed to circumvent thermodynamic limitations, which can direct and inhibit the reversibility of bio-polymerization reactions to accumulate high concentrations of polymerization products in cells[14], as is also observed in the case of polyP accumulation in the *Chlorella* cells (**Figure 2B**). We thus employed the same principles to drive the enzymatic synthesis of solid long-chain polyP from soluble polydisperse polyP, where the phase-transition of the polyP products from soluble to insoluble leads to the favorability of the forward polyP synthesis process in solution. Moreover, the solidity of the long-chain polyP 1,300-mer products facilitates a streamlined, one-step polyP purification procedure *via* simple filtration for downstream use.

The presented microalgal cultivation and extraction procedures at the lab scale also have the potential to be up-scaled to the industrial levels. While microalgal biomass collection,

sonication-based cell disruption, and heating seem to be easily scalable, the centrifugation step required for the insoluble microalgal polyP separation from other cell debris could be one hurdle in the development at large scale due to capacity limitations in centrifugal volume. Therefore, future development of techniques that can facilitate both protease/lipase-based cell lysis to allow us to access the microalgal polyP and membrane-based filtration to separate the microalgal polyP from other cell debris at large scale would be required to bring the long-chain polyP synthesis method into the industrial level. Similarly, the bio-enzymatic procedures to convert polydisperse microalgal polyP into insoluble polyP 1,300-mer have currently been designed as a one-pot, two-step cascade at the lab scale. Future optimization that allows the enzymatic conversion process to upscale would be essential to facilitate long-chain polyP at the industrial scale. For example, the use of magnetic nanoparticles to immobilize the His-tagged enzymes could bypass the need for centrifugation and allow enzyme recycling. Moreover, further investigations into a "panacean" buffer system that could accommodate the required catalytic conditions for all the enzymatic components would allow a one-pot process without any loss in yield.

Given that the polyP-accumulating *Chlorella* spp. is regarded as **G**enerally **R**ecognized **a**s **S**afe (GRAS) by the USA Federal Drug Administration (FDA), the value-added polyP products of various lengths reliably produced by our novel procedure could be used in biomedicine. In particular, polyP products of specific lengths can be used in bone stitches (300–1300-mer), as antivirals (100–300-mer), or as drug delivery vessels (10–100-mer). Moreover, future discovery of the unexplored biological functions or medical applications of purified polyP products of lengths greater than 700-mer (other than bone materials) could also result in greater value for our system. Furthermore, the intermediate creatine phosphate synthesized using the microalgal polyP

could also be used as medicine for heart failure, cardiac surgery, and skeletal muscle hypertrophy [47,48].

Conclusions

Altogether, the catalytic processes established in this study facilitate a sustainable P-bioeconomy platform that can valorize microalgal biomass to produce value-added polyP products at the lab scale. However, a large-scale global sustainable P-bioeconomy is crucial to solving the imminent loss of all global phosphate sources in the next 70 years. Thus, we expect that upon scale-up and further development, the scale of the sustainable P-bioeconomy platform will increase to allow the production of large amounts of high-value polyP materials that are essential for biotechnology and medicine. In particular, as microalgae are abundant in most aquatic ecosystems, an initial application of our polyP synthesis technique in global regions with coasts or rivers that undertake significant phosphorus mineral mining activities would help those regions to divest from economic reliance on phosphorus mineral mining (**SDG 9**). The subsequent establishment of a sustainable P-bioeconomy in other regions lacking phosphorus minerals would help to drive the establishment of local, self-sustainable polyP material production, thereby reducing impacts both of phosphate mineral mining as well as environmental costs related to constant shipping and acquisition of polyP materials.

Acknowledgments

The authors acknowledge Toshikazu Shiba and other employees of RegeneTiss for providing EX-polyP as standard samples, as well as performing HPLC gel-filtration analysis of the synthesized polyP 1,300-mer. P.-H.W. is supported by the National Science and Technology Council of Taiwan (112-2628-E008-005). T.Z.J. is supported by the Japan Society for the Promotion of Science (JSPS) (Grant-in-aid 21K14746) and the Mizuho Foundation for the Promotion of Science. K.F. is supported by an ELSI research grant and NINS Astrobiology Center grant (AB301003 and AB311001).

Author contributions

T.Z.J. and P.-H.W. conceptualized the project and designed experiments. Y.-H.L., S.N., F.-I.,Y., and P.-H.W. performed experiments. All authors contributed to data analysis and interpretation. Y.-H.L., S.N., T.Z.J., and P.-H.W. wrote the manuscript with support from all authors.

Declaration of interests

The authors declare no competing interests.

References

1 A. A. Yaroshevsky, *Geochemistry International*, **44**, 48–55.

2 FAO-Food and A. O. of the United Nations, 2017.
3 Z. Yuan, S. Jiang, H. Sheng, X. Liu, H. Hua, X. Liu and Y. Zhang, *Environmental Science & Technology*, 2018, **52**, 2438–2450.
4 R. Noyes, .
5 Y. Liu, G. Villalba, R. U. Ayres and H. Schroder, *Journal of Industrial Ecology*, 2008, **12**, 229–247.
6 D. W. Schindler, R. E. Hecky, D. L. Findlay, M. P. Stainton, B. R. Parker, M. J. Paterson, K. G. Beaty, M. Lyng and S. E. M. Kasian, *Proceedings of the National Academy of Sciences of the United States of America*, 2008, **105**, 11254–11258.
7 E. Martin, J. Lalley, W. Wang, M. N. Nadagouda, E. Sahle-Demessie and S.-R. Chae, *Chemical Engineering Journal*, 2018, **352**, 612–624.
8 S. Chae, B. Murugesan, H. Kim, D. K. Duvvuru, T. Lee, Y.-H. Choi, M.-H. Baek and M. N. Nadagouda, *ACS ES T Water*, 2021, **1**, 1657–1664.
9 Z. Yuan, S. Pratt and D. J. Batstone, *Current Opinion in Biotechnology*, 2012, **23**, 878–883.
10 A. T. Nielsen, W. T. Liu, C. Filipe, L. Grady Jr, S. Molin and D. A. Stahl, *Applied and Environmental Microbiology*, 1999, **65**, 1251–1258.
11 L. Wang, M. Min, Y. Li, P. Chen, Y. Chen, Y. Liu, Y. Wang and R. Ruan, *Applied Biochemistry and Biotechnology*, 2010, **162**, 1174–1186.
12 A. Lavrinovičs, L. Mežule and T. Juhna, *Algal Research*, 2020, **52**, 102090.
13 S. Eixler, U. Selig and U. Karsten, *Hydrobiologia*, 2005, **533**, 135–143.
14 E. Bondy-Chorney, I. Abramchuk, R. Nasser, C. Holinier, A. Denoncourt, K. Baijal, L. McCarthy, M. Khacho, M. Lavallée-Adam and M. Downey, *Cell Reports*, 2020, **33**, 108318.
15 W. E. G. Müller, H. C. Schröder and X. Wang, *Chemical Reviews*, 2019, **119**, 12337–12374.
16 W. E. G. Müller, E. Tolba, H. C. Schröder and X. Wang, *Macromolecular Bioscience*, 2015, **15**, 1182–1197.
17 W. E. G. Müller, H. Schepler, M. Neufurth, S. Wang, V. Ferrucci, M. Zollo, R. Tan, H. C. Schröder and X. Wang, *Journal of Materials Science and Technology*, 2023, **135**, 170–185.
18 H. Schepler, M. Neufurth, S. Wang, Z. She, H. C. Schröder, X. Wang and W. E. G. Müller, *Theranostics*, 2022, **12**, 18–34.
19 P. Dinarvand, S. M. Hassanian, S. H. Qureshi, C. Manithody, J. C. Eissenberg, L. Yang and A. R. Rezaie, *Blood*, 2014, **123**, 935–945.

20 J. H. Morrissey, S. H. Choi and S. A. Smith, *Blood*, 2012, **119**, 5972–5979.
21 B. Lorenz, J. Münkner, M. P. Oliveira, A. Kuusksalu, J. M. Leitão, W. E. Müller and H. C. Schröder, *Biochimica et Biophysica Acta*, 1997, **1335**, 51–60.
22 J. Roewe, G. Stavrides, M. Strueve, A. Sharma, F. Marini, A. Mann, S. A. Smith, Z. Kaya, B. Strobl, M. Mueller, C. Reinhardt, J. H. Morrissey and M. Bosmann, *Nature Communications*, 2020, **11**, 4035.
23 V. Ferrucci, D.-Y. Kong, F. Asadzadeh, L. Marrone, A. Boccia, R. Siciliano, G. Criscuolo, C. Anastasio, F. Quarantelli, M. Comegna, I. Pisano, M. Passariello, I. Iacobucci, R. D. Monica, B. Izzo, P. Cerino, G. Fusco, M. Viscardi, S. Brandi, B. M. Pierri, G. Borriello, C. Tiberio, L. Atripaldi, M. Bianchi, G. Paolella, E. Capoluongo, G. Castaldo, L. Chiariotti, M. Monti, C. De Lorenzo, K.-S. Yun, S. Pascarella, J.-H. Cheong, H.-Y. Kim and M. Zollo, *Science signaling*, 2021, **14**, eabe5040.
24 T. Z. Jia, P.-H. Wang, T. Niwa and I. Mamajanov, *Journal of Biosciences*, 2021, **46**, 79.
25 M. J. Gray, W.-Y. Wholey, N. O. Wagner, C. M. Cremers, A. Mueller-Schickert, N. T. Hock, A. G. Krieger, E. M. Smith, R. A. Bender, J. C. A. Bardwell and U. Jakob, *Molecular Cell*, 2014, **53**, 689–699.
26 M. Nakagaki, H. Inoue, T. Fujie and S. Ohashi, *BCSJ*, 1963, **36**, 595–599.
27 A. Momeni and M. J. Filiaggi, *Journal of Non-Crystalline Solids*, 2013, **382**, 11–17.
28 D. Wang, Y. Li, H. A. Cope, X. Li, P. He, C. Liu, G. Li, S. M. Rahman, N. B. Tooker, C. B. Bott, A. Onnis-Hayden, J. Singh, A. Elfick, R. Marques, H. J. Jessen, A. Oehmen and A. Z. Gu, *Water Research*, 2021, **206**, 117726.
29 L. Achbergerová and J. Nahálka, *Microbial Cell Factories*, 2011, **10**, 63.
30 K. Motomura, R. Hirota, M. Okada, T. Ikeda, T. Ishida and A. Kuroda, *Applied and Environmental Microbiology*, 2014, **80**, 2602–2608.
31 A. E. Parnell, S. Mordhorst, F. Kemper, M. Giurrandino, J. P. Prince, N. J. Schwarzer, A. Hofer, D. Wohlwend, H. J. Jessen, S. Gerhardt, O. Einsle, P. C. F. Oyston, J. N. Andexer and P. L. Roach, *Proceedings of the National Academy of Sciences of the United States of America*, 2018, **115**, 3350–3355.
32 B. P. Nocek, A. N. Khusnutdinova, M. Ruszkowski, R. Flick, M. Burda, K. Batyrova, G. Brown, A. Mucha, A. Joachimiak, Ł. Berlicki and A. F. Yakunin, *ACS Catalysis*, 2018, **8**, 10746–10760.

33 E. Kozaeva, M. Nieto-Domínguez, A. D. Hernández and P. I. Nikel, *RSC Chemical Biology*, 2022, **3**, 1331–1341.
34 M. Tavanti, J. Hosford, R. C. Lloyd and M. J. B. Brown, *Green Chemistry*, 2021, **23**, 828–837.
35 J. C. Hildenbrand, G. A. Sprenger, A. Teleki, R. Takors and D. Jendrossek, *Microbial Physiology*, 2022, **33**, 1–11.
36 S. Mordhorst, J. Siegrist, M. Müller, M. Richter and J. N. Andexer, *Angewandte Chemie International Edition in English*, 2017, **56**, 4037–4041.
37 P.-H. Wang, K. Fujishima, S. Berhanu, Y. Kuruma, T. Z. Jia, A. N. Khusnutdinova, A. F. Yakunin and S. E. McGlynn, *ACS Synthetic Biology*, 2020, **9**, 36–42.
38 J. C. Hildenbrand, A. Teleki and D. Jendrossek, *Applied Microbiology and Biotechnology*, 2020, **104**, 6659–6667.
39 T. Tumlirsch, A. Sznajder and D. Jendrossek, *Applied and Environmental Microbiology*, 2015, **81**, 8277–8293.
40 C. Mukherjee, C. Mukherjee and K. Ray, *Protoc. Exch.*, , DOI:10.1038/protex.2015.067.
41 R. Ohtomo, Y. Sekiguchi, T. Mimura, M. Saito and T. Ezawa, *Analytical Biochemistry*, 2004, **328**, 139–146.
42 S. Daliry, A. Hallajisani, J. Mohammadi Roshandeh, H. Nouri and A. Golzary, *Global Journal of Environmental Science and Management*, 2017, **3**, 217–230.
43 F.-F. Chu, P.-N. Chu, P.-J. Cai, W.-W. Li, P. K. S. Lam and R. J. Zeng, *Bioresource Technology*, 2013, **134**, 341–346.
44 *J. Biol. Chem.*, 1973, **248**, 4803–4810.
45 D. G. Bolesch and J. D. Keasling, *Journal of Biological Chemistry*, 2000, **275**, 33814–33819.
46 N. H. Williams, *Journal of the American Chemical Society*, 2000, **122**, 12023–12024.
47 E. Strumia, F. Pelliccia and G. D'Ambrosio, *Advances in Therapy*, 2012, **29**, 99–123.
48 D. L. Horjus, I. Oudman, G. A. van Montfrans and L. M. Brewster, *Cochrane database of systematic reviews*, 2011, CD005184.

Tables

Table 1. eQuilibrator-based estimation of the Gibbs free energy ($\Delta_rG'^m$) of the listed enzymatic reactions under the following experimental conditions: 1 mM reactant concentration, pH 7.5, 25°C, pMg 3.0, and 0.25 M ionic strength).

	Reaction	$\Delta_rG'^m$ (kJ/mol)
I	$PolyP_{(n)}$ + ATP → $PolyP_{(n+1)}$ + ADP	~0
II	ADP + Creatine phosphate → ATP + Creatine	−12.2
I + II	$PolyP_{(n)}$ + Creatine phosphate → $PolyP_{(n+1)}$ + Creatine	−12.2

Table 2. The output summary of each step of the one-pot, two-step polyphosphate (polyP) synthesis

670

Step	Substrates	Products	Yield (%)	Residues and Byproducts	Residual polyP yield (%)
A. Synthesis of creatine phosphate from microalgal polyP	Algal polyP, Creatine	Creatine phosphate	95%	Creatine, Algal polyP (< 5-mer)	95%
B. Enzyme removal/pH adjustment	N.A.	N.A.	99%	N.A.	94%
C. Synthesis of long-chain polyP	Creatine phosphate, ATP	Insoluble long-chain polyP 1,300-mer	90%	Creatine	84.6%
D. Filtration	N.A.	N.A.	99%	N.A.	84%
E. Hydrolysis of long-chain polyP	Long-chain polyP 1,300-mer	polyP 100–1,300-mer	90%	P_i	75.5%

671

672